Ecological Processes

RESEARCH

Open Access

Spatiotemporal dynamics of irrigated cropland water use efficiency and driving factors in northwest China's Hexi Corridor

Dandan Du[1,2,3,4], Bo Dong[1,2,3,4*], Rui Zhang[5], Shiai Cui[6], Guangrong Chen[1,2,3,4] and Fengfeng Du[7]

Abstract

Background Agricultural irrigation is an important practice to safeguard crops against drought and enhance grain yield in arid regions. The Hexi Corridor, known as a classic arid region, faces significant pressure on agricultural production and food security due to the scarcity of water resources. There is an urgent need to investigate agricultural water use of the irrigated regions. Water use efficiency (WUE), defined as the ratio of gross primary productivity (GPP) to actual evapotranspiration (ET), serves as a valuable indicator linking carbon assimilation and water loss. It enables the quantification of areas where water can be utilized more effectively. However, the long-term spatiotemporal dynamics of WUE and driving mechanism in the irrigated areas of the Hexi Corridor remain unclear.

Results This study used GPP calculated by a light use efficiency model (EF-LUE), ET estimated by an ETMonitor model and irrigated cropland maps across China (IrriMap_CN) to examine the spatiotemporal dynamics of irrigated cropland WUE and its controlling factors in the Hexi Corridor from 2001 to 2018. The results are as following: (1) The average annual WUE was approximately 1.34 ± 0.38 g C kg^{-1} H_2O yr^{-1}, with an increasing trend of 0.012 g C kg^{-1} H_2O yr^{-1}, and faster growth observed during 2011–2018 compared to 2001–2010. (2) The contribution of GPP to WUE trends and WUE interannual variability (IAV) was greater than that of ET. (3) The dominant climatic factors of WUE IAV in the Hexi Corridor were SPEI, precipitation, and soil moisture. (4) The standardized Structural Equation Model (SEM), incorporating the relationship between WUE and factors such as water, energy, NDVI, and water-saving irrigation, explained 81% of the variation in irrigated cropland WUE. Here, biological factors (GPP and NDVI) were the primary factors influencing WUE variability, and water-saving irrigation had a stronger indirect effect than climate factors (water and energy) on variation in WUE.

Conclusions Our findings offer valuable theoretical insights into the mechanisms governing the interaction between the carbon and water of irrigated cropland, guiding the management of water resources and land in agricultural practices within the Hexi Corridor.

Keywords Irrigated cropland, Water use efficiency, Hexi Corridor, Interannual variability, Dominant factor, Driving mechanism

*Correspondence:
Bo Dong
dongbobby@163.com
Full list of author information is available at the end of the article

Background

Agriculture is a significant consumer of water, and its use continues to increase globally with a growing world population. According to the Food and Agricultural Organization's (FAO) report, agricultural water demand is projected to increase by approximately 35% to sustain the needs of an estimated 10 billion people worldwide by 2050 (FAO 2021). Besides, climate change has exacerbated the frequency and intensity of droughts, contributing to the depletion of freshwater resources over the past few decades (Grafton et al. 2013). Because of increasing demands and significant reductions for freshwater resources, water disputes persist in many parts of the world, especially in arid regions. Water efficiency for food production remains low and unsatisfactory, leading to environmental degradation such as groundwater over-exploitation, reduced river runoff, wildlife habitat destruction and environmental pollution (United Nations 2021). Therefore, achieving water savings in current agricultural practices is imperative for addressing global food and water security (Zhou et al. 2021).

Water use efficiency is a vital indicator for evaluating water consumption and dry matter production (Keenan et al. 2013; Sun et al. 2018). Initially, crop physiologists defined water use efficiency (WUE) at leaf-scale as the quantity of carbon assimilation and crop yield per unit transpiration (Linderson et al. 2012; Reichstein et al. 2007). At the ecosystem level, WUE is generally described as the ratio of gross primary productivity (GPP) to actual evapotranspiration (ET) (Bonan 2008; Fischer and Turner 1978; Ji et al. 2023). Cropland WUE describes the relationship between water use and crop production, and it is a widely used indicator for decision-making in agricultural water management (Zhou et al. 2021). Over the past decade, numerous studies have examined the WUE of cropland for various crop types and the changes in WUE under different agronomic practices (e.g., irrigation, fertilization, conservation tillage, plastic film mulching, etc.) at the field scale. Pan et al. (2024) investigated how water-nitrogen interaction impacts water and nitrogen use efficiency in seed maize. Zhang et al. (2019b) examined the effect of water stress on photosynthesis and WUE of common reed. Fan et al. (2019) studied whether film fully-mulched ridge–furrow water harvesting sustainably improves WUE of corn.

With the advancement of information and remote sensing technologies, an increasing number of researchers have conducted some global comprehensive and modeling endeavors to evaluate the spatial distribution, trend and drivers of agroecosystem WUE in the long-term continuous scale using remote sensing data (Ai et al. 2020; Wang et al. 2021). The study from Wang et al. (2018a) revealed the great potential in remotely retrieving variability in cropland WUE using time-series MODIS NDVI data across large regions. The study by Zhao et al. (2021) characterized the spatial temporal variability of cropland WUE in China using the satellite-retrieved data, and discovered the significantly increasing trend between 1982 and 2017. Bai et al. (2020) found WUE in dryland ecosystems in China was strongly influenced by precipitation based on eddy covariance and remote sensing data. Remote sensing-based ecosystem models have provided powerful tools for monitoring the dynamics of cropland WUE at regional and global scales.

Variations in WUE are the combined result of changes in GPP and ET. It is well known that climate change has significantly affected the relationship between GPP and ET, thus impacting WUE (Huang et al. 2015). Circumstances such as water resource shortages and extreme environmental conditions, like drought and intense precipitation, affect regional carbon and water cycles (Wang et al. 2017). For example, Zhu et al. (2011) showed that water resource restriction affected WUE, with WUE decreasing in different ecosystems as the evaporation ratio increases. Besides, the trend of WUE in relation to climate change will likely vary under different conditions, such as dry and wet environments (Liu et al. 2015; Yu et al. 2007; Zhang et al. 2012). In addition to climate, anthropogenic activities, such as urbanization, irrigation, and fertilization, could also directly impact ecosystem GPP and ET (Yang et al. 2022a). Discrepancies in agricultural management practice for crops among arid and highly arid climate zones can lead to the discrepancies of WUE (Wang et al. 2021). Previous studies have shown that cropland WUE is influenced by various factors such as climate, environmental conditions, crop type, and agronomic management practices (Hu and Lei 2021). However, most studies investigating interannual variations in cropland WUE and their driving mechanisms over a large-scale, long-term continuous period have primarily focused on climate factors, while often overlooking agronomic management practices, particularly the impact of irrigation. Yang et al. (2022b) investigated the interannual dynamics of cropland WUE and its response to climate variations in single and double cropping systems across China, without distinguishing rainfed and irrigated regions. The study from Yang et al. (2023) analyzed the impact of cropland change on WUE in the Hexi Corridor, but their study did not consider the change in irrigated area. By using Global Food Security Support Analysis Data (GFSAD) to obtain global rainfed and irrigated regions for the nominal year 2015, Ai et al. (2020) assessed WUE in rainfed and irrigated cropland during 2000–2014. However, their study did not account for annual changes in irrigated areas. Irrigation is an important agronomic management practice that

simultaneously regulates photosynthesis and ET. There is a general imperative to conduct on the dynamics of irrigated cropland WUE and its driving factors in dryland cropland ecosystems, not only because it is critically important for improving water-saving irrigation management of the dryland cropland ecosystems, and also for future food security in light of frequent climate anomalies (Bai et al. 2020; Wang et al. 2018a; Yu et al. 2018).

The Hexi Corridor is a typical arid region that experiences abundant light and heat but has limited water resources, receiving less than 200 mm of rainfall annually with significant variation throughout the year (Fig. 1). Due to climate change, extreme environmental conditions (e.g., drought, heat wave and extreme precipitation) are becoming increasingly frequent (Su et al. 2007). Agriculture in the region relies heavily on irrigation, mainly sourced from streamflow and groundwater (Bao and Fang 2007). The human-made agricultural oases are essential regions for food production in the Hexi Corridor (Wang et al. 2021; Yang et al. 2020). Meanwhile, the region faces severe water scarcity issues, posing a limiting factor for regional prosperity and economic development (Kang et al. 2017). In particular, the government has launched several water-saving irrigation projects in the past 20 years, involving expanding water-saving irrigation areas in large and medium-sized irrigation areas (Tian et al. 2020), as well as adjusting planting structures based on local conditions (GPWRB 2007). Tian et al. (2020) showed how climatic factors and human activities simultaneously regulated photosynthesis and ET in the Shiyang River basin, and found the relative contribution of human activities in the water-saving project (WSP) to ET was 77.5%, while that of climate factors was 22.5%. Nevertheless, research on the long-term interannual variation of WUE in irrigated areas of the Hexi Corridor and its response to climatic factors, as well as the water-saving irrigation, is scare. This has limited our comprehension of water-carbon interactions in the region, especially regarding the potential application of effective cropland management and efficient water utilization protocols.

For this study, we utilized GPP and ET data previously estimated by the EF-LUE and ETMonitor models, which have demonstrated superior performance in capturing the spatial variation of GPP and ET in irrigated cropland regions than other global GPP and ET products, e.g., the MODIS and PML-V2 products. The annual irrigated cropland maps across China (IrriMap_CN) were used to determine the irrigated area. The main aims of this study are to (1) evaluate temporal and spatial dynamics of irrigated cropland WUE in the Hexi Corridor; (2) quantify the roles of GPP and ET in controlling cropland WUE; (3) analyze dominant factors of cropland WUE interannual variability (IAV); (4) illustrate driving mechanism of WUE based on Bayesian structural equation model.

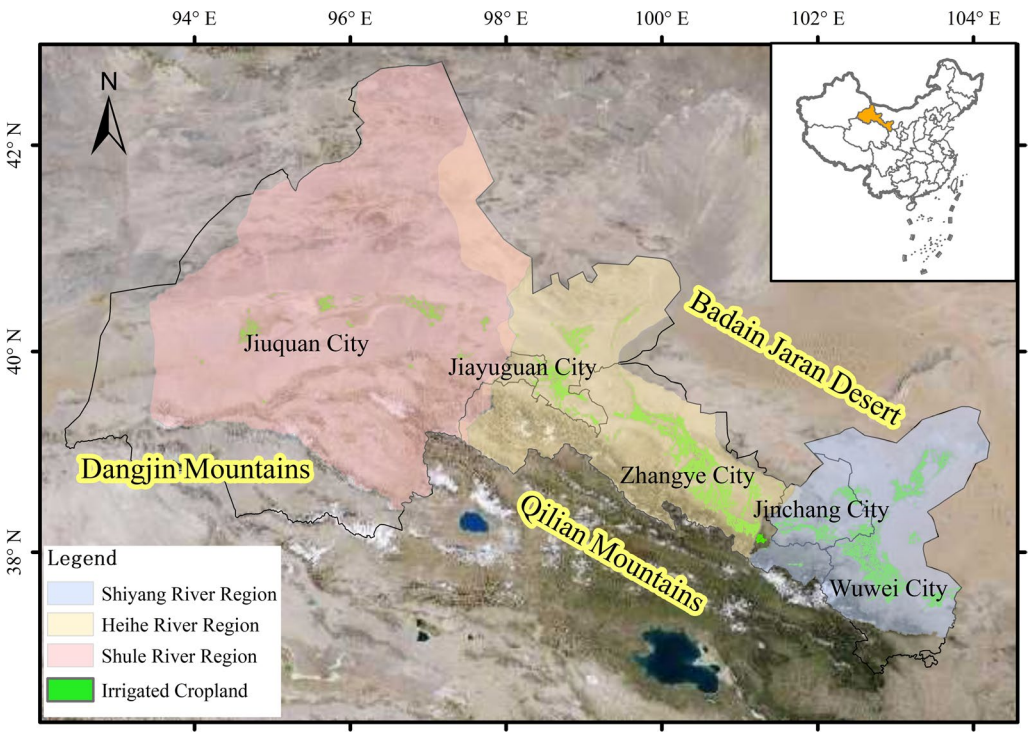

Fig. 1 The subregions and pattern of unchanged irrigated cropland in the Hexi Corridor during 2001–2018

Materials and Methods

Study area

The Hexi Corridor positioned in northwest of China (37°17′−42°48′ N, 93°23′−104°12′ E), west of the Yellow River, between the Qilian Mountains and the Badain Jaran Desert (Fig. 1). It is a narrow strip of land running northwest-southeast. This region has a typical arid climate and falls under the temperate and warm temperate continental climate zones. The Qilian Mountains are the origin of three significant inland rivers, namely, the Shiyang River, the Heihe River, and the Shule River, which give rise to oasis irrigation areas of approximately 2.2×10^5 km^2 (Li et al. 2016). The human-made agricultural oases are vital regions for food production, with the main crops cultivated including wheat, corn, oil-bearing crops, vegetables, orchards, cotton, and tubers. According to the 2019 Gansu Water Resources Bulletin, irrigation cropland accounts for 72.58% of the entirety of cultivated land in the inland river basin, and irrigation water use accounts for more than 80% of total water consumption (HBGP 2019). In order to meet the large water demand, groundwater is used to supplement water resources to irrigate croplands in the Hexi Corridor. Nevertheless, over-exploitation of groundwater has resulted in severe ecological degradation of oases (Feng et al. 2015, 2019). The Chinese government has launched a variety of comprehensive rehabilitation projects within inland river basins such as water-saving irrigation projects to preserve the regional ecological environment and support sustainable economic and social development.

Data

The details of several datasets used in this study are described in the following sections (Table 1).

ET and GPP data

In this study, we used ET data based on a combined model with multi-process parameterizations retrieved from satellite observations (Named ETMonitor), with a spatial resolution of 0.0083°×0.0083°, covering the period 2001–2019 (Zheng et al. 2022, 2016). The ETMonitor has been calibrated against ground flux observations and has performed significantly better in capturing the spatial variations of ET in irrigated cropland regions than other global ET products (Hu and Jia 2015; Sriwongsitanon et al. 2020; Weerasinghe et al. 2020).

The GPP data utilized in this research were derived using a light-use-efficiency model specifically designed for estimating GPP in agroecosystems, known as EF-LUE. This model incorporates the evaporative fraction (EF) estimated from the ETMonitor model as a constraining factor and the model parameters were optimized for different climatic zones using CO_2 flux measurements from crop sites (Du et al. 2022).

Irrigated cropland data

Irrigated cropland data utilized in this study were sourced from Zhang et al. (2022). They obtained annual irrigated cropland maps across China (IrriMap_CN) at a resolution of 500 m spanning from 2000 to 2019 by using a machine-learning method (Zhang et al. 2022). It achieved high accuracy, ranging from 77.2% to 85.9%, based on the validation of more than 3000 ground truth points. We extracted GPP, ET and WUE in irrigated croplands derived from the annual crop cover data provided by IrriMap_CN.

Climate, soil moisture and other auxiliary data

Annual 1 km resolution average temperature and accumulated precipitation data in China from National Earth

Table 1 The details of several datasets used in this study

Variable	Dataset/model	Resolution	Data availability	Reference
GPP	EF-LUE model	1 km	2001–2019	(Du et al. 2022)
ET	ETMonitor model	1 km	2000–2019	(Zheng et al. 2022)
Irrigated cropland	IrriMap_CN	500 m	2000–2019	(Zhang et al. 2022)
Temperature	Bilinear interpolation	1 km	1982–2022	(Peng et al. 2019)
Precipitation				
Radiation	GLASS	0.05°	2000–2022	(Zhang et al. 2016)
SPEI	Random forest	1 km	2001–2020	(Xia et al. 2023)
Soil moisture	Random forest	1 km	2000–2020	(Zheng et al. 2023)
Wind speed	CFMD	0.1°	1979–2018	(He et al. 2020)
Humidity				
Pressure				
NDVI	MOD13A2	1 km	2000–Present	(Didan and Barreto Munoz 2019)

System Science Data Center, National Science & Technology Infrastructure of China (http://www.geodata.cn accessed 8 March 2024). It adjusted a monthly temperature and precipitation dataset from Peng et al. (2019) to an annual scale. The original monthly dataset was spatially downscaled from the 300 Climatic Research Unit (CRU) dataset using the climatology dataset of WorldClim.

Downward Shortwave Radiation (DSR) data from the Global Land Surface Satellite (GLASS) DSR product, which has a resolution of 0.05 and global DSR based on MODIS and AVHRR data (Zhang et al. 2014, 2019a). The AVHRR data were calculated using an improved lookup table algorithm, while the MODIS data were calculated using a hybrid algorithm (Zhang et al. 2016). We resampled data to 1 km using bilinear interpolation method (Wong et al. 2004).

A resolution of 1 km/monthly soil moisture data from National Tibetan Plateau/Third Pole Environment Data Center. The dataset was derived from the European Space Agency-Climate Change Initiative (ESA-CCI) surface soil moisture combined product at a resolution of 0.25° by using Random Forest algorithm (Zheng et al. 2023).

The standardized precipitation evapotranspiration index (SPEI) data used in this study were obtained from Xia et al.'s (2023) research. They developed a high-precision machine learning algorithm to calculate grid-based SPEI at a 1 km resolution across multiple time scales (1 month, 3 months, 6 months, 12 months, and 24 months) over a large regional area, spanning from 2001 to 2020.

Other meteorological data like wind speed, humidity and pressure were taken from China Meteorological Forcing Dataset (CFMD), which provides near-surface meteorological data over China with a temporal/spatial resolution of three hours/0.1°, covering the period of 1979–2018. This dataset was constructed by fusing multisource data, including remote sensing products, reanalysis datasets, and station observation data. The CFMD has undergone a validation against station observations, which demonstrated its superior performance compared to the Global Land Data Assimilation System (GLDAS) (He et al. 2020). Because of the relative coarse resolution of the data, we just used the statistical values with the temporal and spatial scales of year/0.1° at the basin level rather than pixel level.

The study utilized MOD13A2 Normalized Difference Vegetation Index (NDVI) data, which offer continuity indices on a per-pixel basis at a spatial resolution of 1 km (km) (https://search.earthdata.nasa.gov/ accessed 14 March 2024).

Additionally, water-saving irrigation area data from 2001 to 2018 in the Hexi Corridor were taken from the Water Resources Bulletin of Gansu Province. The water-saving irrigation area refers to the area where water-saving measures such as drip irrigation, micro-irrigation, and low-pressure pipe irrigation are implemented. By using the advanced equipment and means during crop irrigation, water consumption can be reduced while still meeting the water requirements of crops. Interannual variation of water-saving irrigation area can reflect the variation of local irrigation level in the context of implementing water-saving irrigation projects to a certain extent. Therefore, we used the total area of water-saving irrigation as the irrigation factor in the SEM model. Data on the area of major crops in different regions were sourced from the Gansu Development Yearbook 2019.

Methods

At the ecosystem level, WUE was typically described as the ratio of GPP to actual ET, as expressed by (Sun et al. 2018):

$$WUE = \frac{GPP}{ET} \tag{1}$$

Trend analysis and mutation test

Trend analysis were performed using the Theil-Sen estimator (Sen 1968) which calculates the slopes of all lines between each pair of points. Subsequently, the median of all computed slopes is utilized for the line-fitting process. This method is highly robust and has greater resilience against outliers than the simple linear regression method (Wilcox 2010).

$$\theta = Median\left(\frac{X_j - X_i}{j - i}\right) \forall_j > i \tag{2}$$

where X is the value of variable in the year, i and j represent the serial number of years. The result (θ), which is greater than 0, indicates an increase in the variable. Conversely, a value less than 0 represents a decrease in the variable.

To identify the abrupt change points of the WUE time series from 2001–2018, the non-parametric Mann–Kendall (M–K) mutant test was employed. This entails finding the intersection between a forward sequence (UF) of annual WUE and a backward sequence (UB) of the inversion of annual WUE with a confidence level indicating statistical significance at $P < 0.05$. This approach is useful in detecting abrupt changes (Wang et al. 2020; Xu et al. 2018; Yang and Yang 2012; Yang et al. 2022a).

Roles of GPP and ET in controlling cropland WUE

This study used a differential equation to quantify the contribution of GPP and ET to the long-term trend

of WUE (Yang et al. 2022b). According to Eq. (1), the first-order differential approximation can be estimated as follows:

$$\frac{dWUE}{dt} = \frac{\partial WUE}{\partial GPP} \times \frac{dGPP}{dt} - \frac{\partial WUE}{\partial ET} \times \frac{dET}{dt} + \varepsilon \tag{3}$$

∂WUE/∂GPP and ∂WUE/∂ET represent WUE changes resulted from per unit of GPP or ET, respectively (Wang et al. 2020). ε is the system error in the contribution estimation. The relative contributions of GPP and ET to WUE trend can be expressed as follows (Yang et al. 2022b):

$$C(GPP) = \frac{\partial WUE}{\partial GPP} \times \frac{dGPP}{dt} \tag{4}$$

$$C(ET) = -\frac{\partial WUE}{\partial ET} \times \frac{dET}{dt} \tag{5}$$

$\frac{dWUE}{dt}$, $\frac{dGPP}{dt}$ and $\frac{dET}{dt}$ are estimated as the slopes of linear regression for WUE, GPP, and ET against time (t) based on the least square method, respectively.

Furthermore, the individual proportional contribution of GPP (Eq. (4)) and ET (Eq. (5)) to the WUE trends can be represented as follows (Yang et al. 2022b):

$$R_{GPP} = \frac{\mathrm{C(GPP)}}{\mathrm{C(GPP)} + \mathrm{C(ET)}} \times 100\% \tag{6}$$

$$R_{ET} = \frac{\mathrm{C(ET)}}{\mathrm{C(GPP)} + \mathrm{C(ET)}} \times 100\% \tag{7}$$

Relative importance analysis

The Lindeman–Merenda–Gold (LMG) method is a recommended method which has been used in many published papers to evaluate the relative importance of correlated input regressors by R^2 decomposition in a multiple linear model (Groemping 2006). By utilizing unweighted averages across sequential R^2 values for each variable in all permutations of regressors, this metric mitigates order effects. Furthermore, the total R^2 is decomposed into non-negative components (Yao et al. 2017). We used calc.relimp function in R package to calculate relative importance metrics for the linear model. The recommended metric is 'lmg', vector of relative contributions obtained from the LMG method, which is the contribution averaged over orderings among regressors (Lindeman et al. 1981). In this study, we first standardized the data and applied LMG method to differentiate the contribution of GPP and ET to WUE IAV in irrigated croplands. And then we further investigated driving factors of cropland WUE IAV based on LMG method. The climatic factors including temperature, precipitation, radiation, soil moisture, drought index (SPEI), and biological factor (NDVI) were considered during the relative importance analysis.

Bayesian structural equation modeling

Bayesian structural equation models (SEMs) are powerful models to access interrelationships among observed and latent variables (Lee and Song 2014). SEM offers a method to partition the net effect into direct and indirect effects. It allows environmental variables to interact, rather than isolating a single controlling factor from others like other traditional regression analysis (Wang et al. 2018b). Many variables affect WUE as an offset or correlation to its impact on both GPP and ET. To avoid collinearity among variables, we used precipitation, soil moisture and SPEI to reflect water condition while temperature, solar radiation, humidity, wind speed and pressure to reflect energy condition. NDVI was used to reflect biological factors such as the condition of crops, and NDVI was also affected by water and energy. In addition, water-saving irrigation area data were considered to reflect the effect of human irrigation management to WUE. In the Hexi Corridor, low precipitation levels often fail to meet water requirements of crops, making irrigation essential for crop growth and production. Additionally, irrigation water losses from evaporation occurring on bare soil, which are not correlated with productivity, tend to decrease WUE (Sun et al. 2015). Irrigation is primarily regulated by anthropogenic water-saving measures aimed at reducing water loss (Tian and Zhang 2020). Agriculture irrigation management has modified the allocation of water resources and adjust strategies for water utilization in drylands, thereby influencing the cropland WUE (Wang et al. 2021).

Before constructing and analyzing the Bayesian SEM model, the data were standardized to ensure that the influences of different variables on the model results have equal weights. Bayesian SEM was created using PyMC3 package in Python and run with four Markov chain Monte Carlo (MCMC) chains with 1000 iterations. The MCMC results indicated that Gelman-Rubin values (R_hat, the ratio of the effective sample size to the overall number of iterations) were close to one, suggesting convergence of the MCMC chain. The larger effective sample sizes (ESS) (ess_mean > 2000 for all coefficient estimates) ensure adequate estimation of the parameters. The estimate of coefficient represents direct effects (also called path coefficient) and indirect effects were estimated by multiplying the direct effects (Yan et al. 2023).

Results

Spatial pattern of WUE

The spatial distribution of mean annual WUE of irrigated cropland for 2001–2018 in the Hexi Corridor are presented in Fig. 2 (left). The multiyear mean WUE showed apparent regional heterogeneity and varied from 0.07 g C kg^{-1} H_2O yr^{-1} to 2.42 g C kg^{-1} H_2O yr^{-1}, with mean value of 1.34 ± 0.38 g C kg^{-1} H_2O yr^{-1}. The high value of WUE (> 2 g C kg^{-1} H_2O yr^{-1}) occurred in the Heihe River basin (Ganzhou District), which only accounted for 3.36% of croplands. The area of high WUE had high GPP (> 1250 g C m^{-1} yr^{-1}) but moderate ET (600–700 mm yr^{-1}) (Figure S1). The relatively high WUE (> 1.6 g C kg^{-1} H_2O yr^{-1}) mainly distributed in the Heihe River basin (Linze County, Gaotai County, Suzhou District) and the Shiyang River basin (Liangzhou District, Yongchang County). The area of low WUE (< 0.8 g C kg^{-1} H_2O yr^{-1}) account for 9.25%, mainly distributed in the upper Heihe River basin and the Shiyang River basin. About 42.68% of the total irrigated croplands had WUE values ranging from 1.2 to 1.6 g C kg^{-1} H_2O yr^{-1}.

At the basin level (Fig. 2 right), the Heihe River basin had the highest WUE (1.41 ± 0.41 g C kg^{-1} H_2O yr^{-1}) which attributed to the higher mean value of GPP but lowest ET. The Shule River basin and the Shiyang River basin had the similar WUE values, with mean WUE of 1.28 ± 0.29 g C kg^{-1} H_2O yr^{-1} and 1.29 ± 0.36 g C kg^{-1} H_2O yr^{-1}, respectively. The Shiyang River basin had relatively higher GPP and ET. The Shule River basin had highest ET among three basins.

Temporal trend of WUE

The temporal trend of irrigated cropland WUE from 2001 to 2018 in the Hexi Corridor showed spatial variations (Fig. 3a). Overall, approximately 80.83% of the total irrigated cropland area showed an increase in WUE. The area of Theil-Sen slope higher than 0.03 accounted for 27.06%, which indicated larger increasing trends of WUE, primarily observed in the middle reaches of the Heihe River basin (such as Shandan County, Minle County, Ganzhou District) and the Shiyang River basin (such as Jinchuan County, Gulang County). The negative trend in WUE was primarily observed in the Shiyang River basin (Liangzhou District and Minqin County), a few areas in the upper-middle reaches of the Heihe River basin (Ganzhou District and Gaotai County), and the Shule River basin (Dunhuang City).

Additionally, the M–K test method was used to identify the point of change of annual WUE from 2001 to 2018, we found that WUE underwent a significant shift in 2011 (Fig. 3b). Thus, the whole period was separated into two period which WUE showed an increasing trend of 0.004 g C kg H_2O yr^{-1} from 2001 to 2011 and 0.006 g C kg H_2O yr^{-1} from 2011 to 2018, respectively (Fig. 3c). In general, WUE experienced a mean increasing

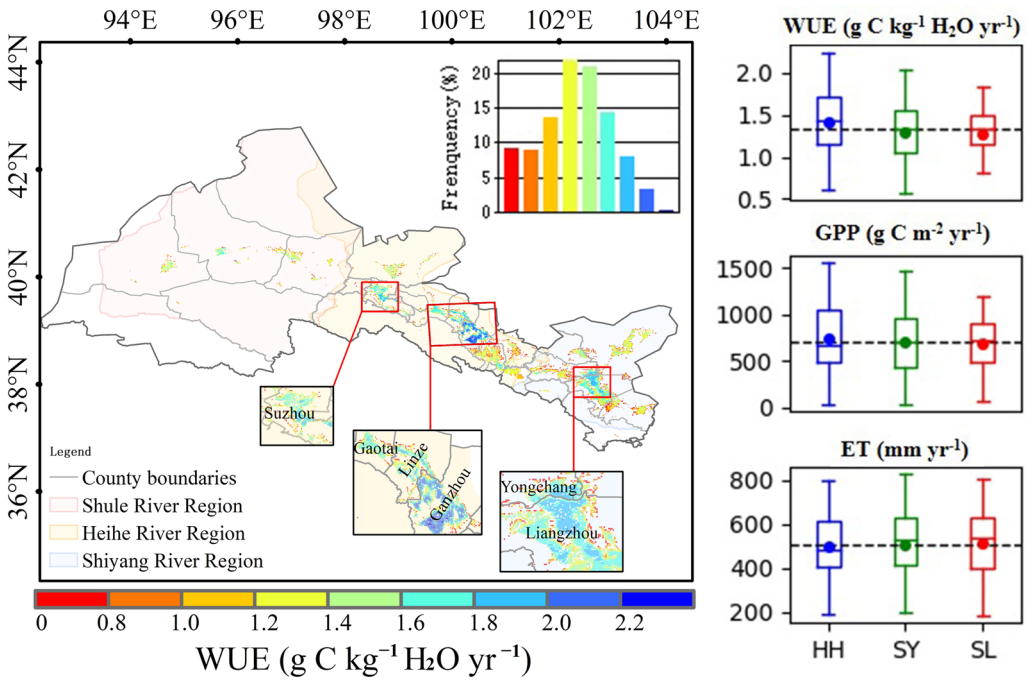

Fig. 2 The spatial distribution of mean annual WUE in irrigated croplands for 2001–2018 and the variation of irrigated cropland GPP, ET and WUE among the Heihe River basin (HH), the Shiyang River basin (SY), and the Shule River basin (SL)

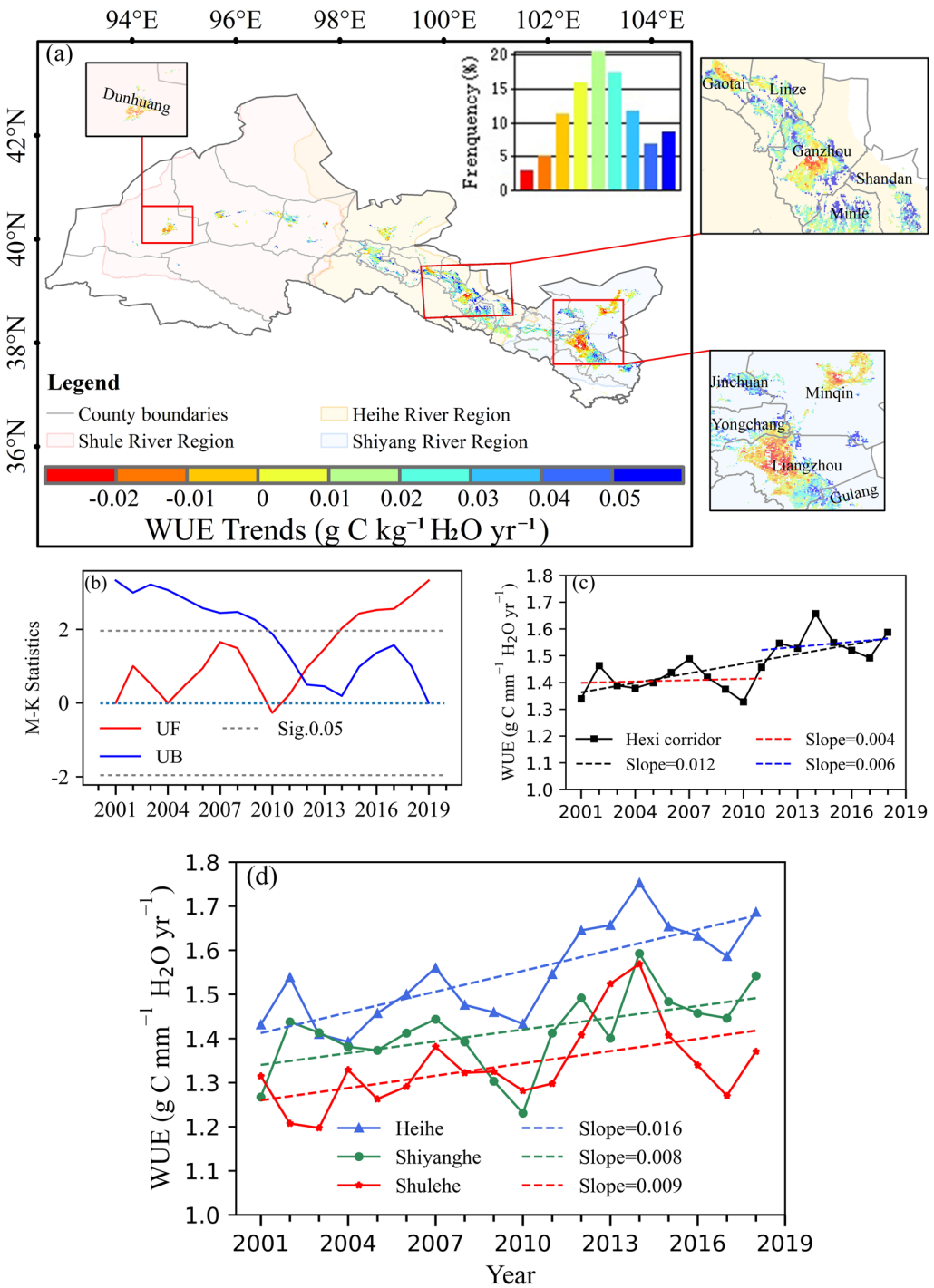

Fig. 3 **a** The spatial distribution of annual WUE trends in irrigated croplands for 2001–2018. **b** M – K mutation test of annual WUE from 2001 to 2018. **c** The time series of irrigated cropland WUE and trends during the period of 2001–2011 and 2011–2018 in the Hexi Corridor. **d** The time series of irrigated cropland WUE in the Heihe River basin, the Shiyang River basin, and the Shule River basin

trend of 0.012 g C kg H_2O yr^{-1}, which resulted in an overall increase of 7.89% from 2001 to 2018.

As shown in Fig. 3d, WUE varied significantly between the basins, with the average WUE in the Heihe River basin (0.016 g C kg H_2O yr^{-1}) being higher than that in the Shiyang River basin (0.009 g C kg^{-1} H_2O yr^{-1}) and the Shule River basin (0.008 g C kg^{-1} H_2O yr^{-1}). Over the 18-year period, the rate of increase in WUE was

highest in the Heihe River basin (12.87%), followed by the Shiyang River basin (4.07%) and the Shule River basin (3.04%).

Roles of GPP and ET in controlling cropland WUE

In general, irrigated cropland GPP and ET showed increasing trends in the Hexi Corridor during the period of 2001–2018, with the average trend of 10.937 g C m^{-2} yr^{-1} and 2.785 mm yr^{-1}, respectively (Fig. 4). The contribution of GPP to WUE trends [C(GPP) = 0.026] was greater than that of ET [C(ET) = 0.009]. The similar result was also found at the basin level. However, the contributions of GPP and ET to WUE trends were different among basins. The highest contribution of ET to WUE trend occurred in the Shule River basin [C(ET) = 0.010] while the highest contribution of GPP to WUE trend occurred in the Heihe River basin [C(GPP) = 0.032], and both GPP and ET showed the lowest contribution values to WUE trend in the Shiyang River basin [C(GPP) = 0.021, C(ET) = 0.006]. In addition, the Heihe River basin had a highest WUE increasing trend (0.023 g C kg H_2O yr^{-1}) induced by a significantly increasing trend of GPP (13.078 g C m^{-2} yr^{-1}) and relatively weakly increasing trend of ET (2.783 mm yr^{-1}).

In order to analyze the roles of GPP and ET in determining the spatial pattern of irrigated cropland WUE trends, a composite map of WUE, GPP and ET trends was created (Fig. 5a). Among irrigated croplands with increasing trends of WUE, approximately 61.86% of the irrigated croplands had increasing trends of both GPP and ET (light green in Fig. 5a) while 13.33% of irrigated croplands had increasing trends of GPP but decreasing trends of ET (blue in Fig. 5a), which mainly occurred in the middle reaches of the Heihe River basin. About 12.54% of irrigated croplands showed decreasing trends of WUE, GPP and ET which mainly distributed in the middle reaches of the Heihe River (Ganzhou District and Gaotai County) and part of the Shiyang River Basin (Liangzhou District, Minqin County, etc.) (pink in Fig. 5a). Irrigated croplands with decreasing trends of WUE but increasing trends of ET and GPP only accounted for about 4.13% which mainly observed in the Shule River basin (red in Fig. 5a).

We further compared the contribution of GPP and ET to irrigated cropland WUE trends (Fig. 5b). The most

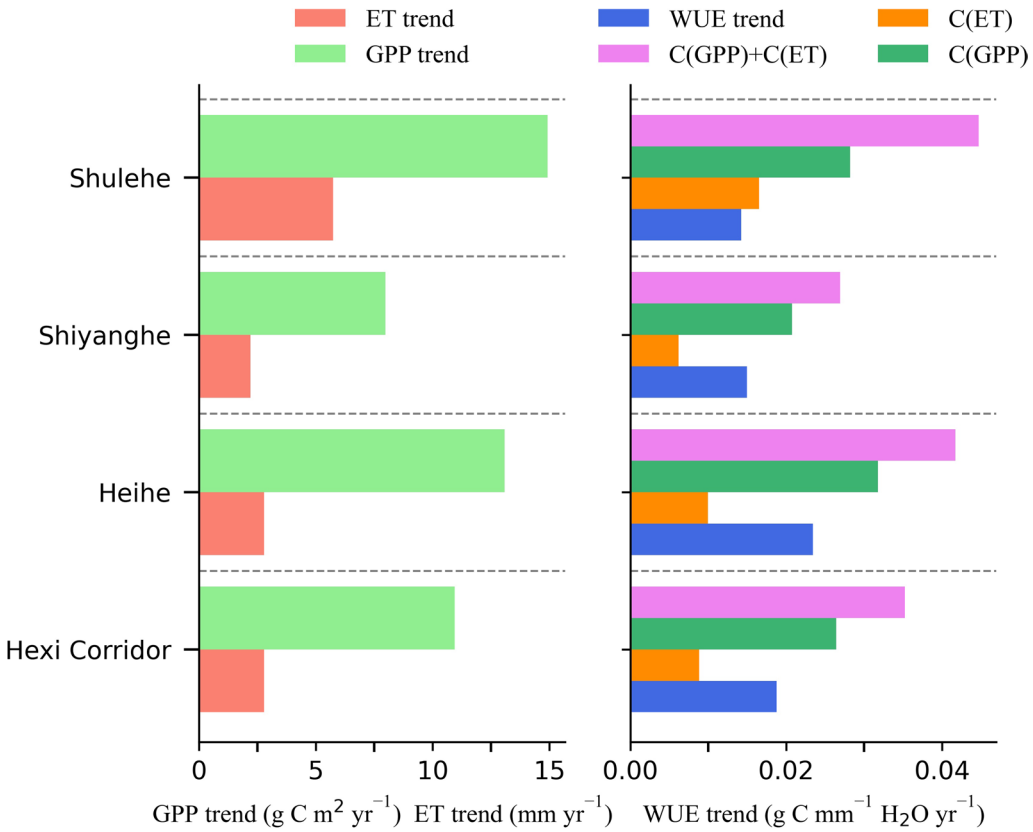

Fig. 4 GPP trend, ET trend, WUE trend as well as the contributions of GPP [C(GPP)] and ET [C(ET)] to WUE trend in irrigated croplands during 2001–2018 in the whole Hexi Corridor and three basins

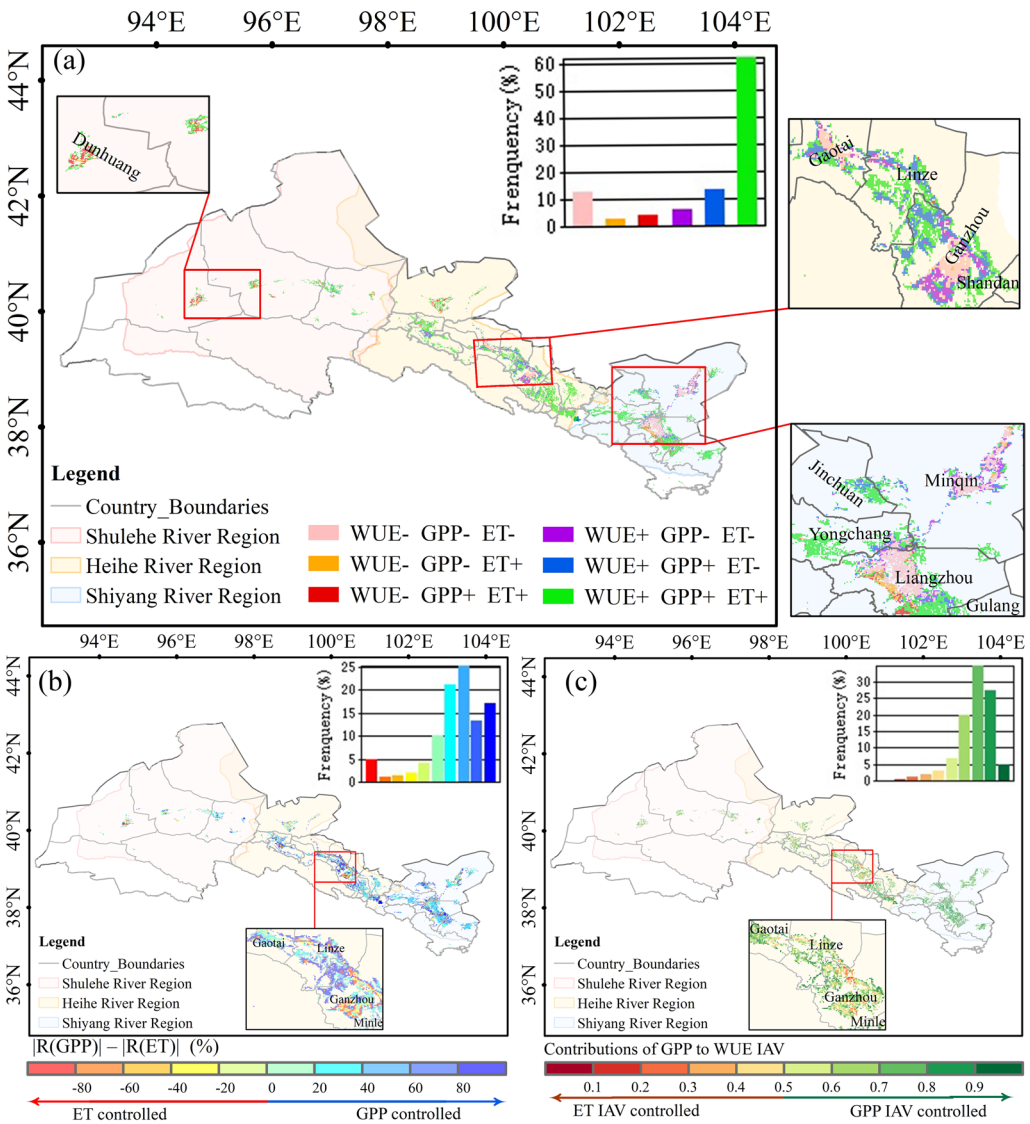

Fig. 5 **a** The composite map of WUE, GPP and ET trends, **b** the spatial pattern of the difference in absolute contributions of GPP and ET to WUE trends, and **c** contributions of GPP to WUE IAV for irrigated croplands in Hexi Corridor over 2001–2018. (The symbol '+' (or '–') in (**a**) means positive (or negative) trend of WUE, GPP and ET. The symbol 'GPP controlled' in (**b**) and 'GPP IAV controlled' in (**c**) indicate absolute values of the relative contribution of GPP is higher than that of ET

area of irrigated croplands (about 86.79%) were controlled by GPP (|R(GPP)| > |R(ET)|), which indicated that GPP played dominant roles in the temporal trends of WUE in most regions. Contributions of GPP and ET to WUE IAV also estimated by LMG method and the relative importance metrics are normalized to sum to 1 (the sum of contributions of GPP and ET to WUE IAV is 1). The relative contribution of GPP to WUE IAV was shown in Fig. 5c. There were about 73.7% irrigated cropland area where WUE IAV was controlled by GPP variation, indicating that GPP also predominantly influenced WUE IAV in most regions. Area where ET dominated WUE trends and IAV were primarily concentrated in small regions within the Heihe River basin (Ganzhou District, Linze County).

Dominant factors of cropland WUE IAV

Temperature, precipitation and solar radiation are critical climatic driving factors for both photosynthesis and transpiration that can affect changes in WUE. In order to illustrate their impacts on irrigated cropland WUE IAV, pixel-wise relative importance analysis was adopted in this study. The relative importance metrics were depicted in a cyan-magenta-yellow

(CMY) triangular figure, representing precipitation (cyan), radiation (magenta) and temperature (yellow) (Fig. 6a). The dominant climatic factors of WUE IAV varied across the Hexi Corridor. There were relative more areas where precipitation was the predominant factor of WUE IAV. Temperature dominated area mainly occurred in Minqin County of the Shiyang River basin while radiation dominated area mainly occurred the middle reaches of the Heihe River basin (Shandan County, Minle County) and Yongchang County of the Shiyang River basin.

However, the overall proportion of variance (the coefficients of determination for multiple linear models) explained by model based on three regressors (precipitation, radiation and temperature) were low in most regions (Fig. 6b). In addition, we further added SPEI indices and soil moisture data to consider the impact of drought and wet conditions on WUE IAV. SPEI indices were calculated with mean of multiple time scales (see Sect. "Climate, soil moisture and other auxiliary data" for data description). Besides, NDVI was used to reflect biological factors such as the condition of crops. The coefficients

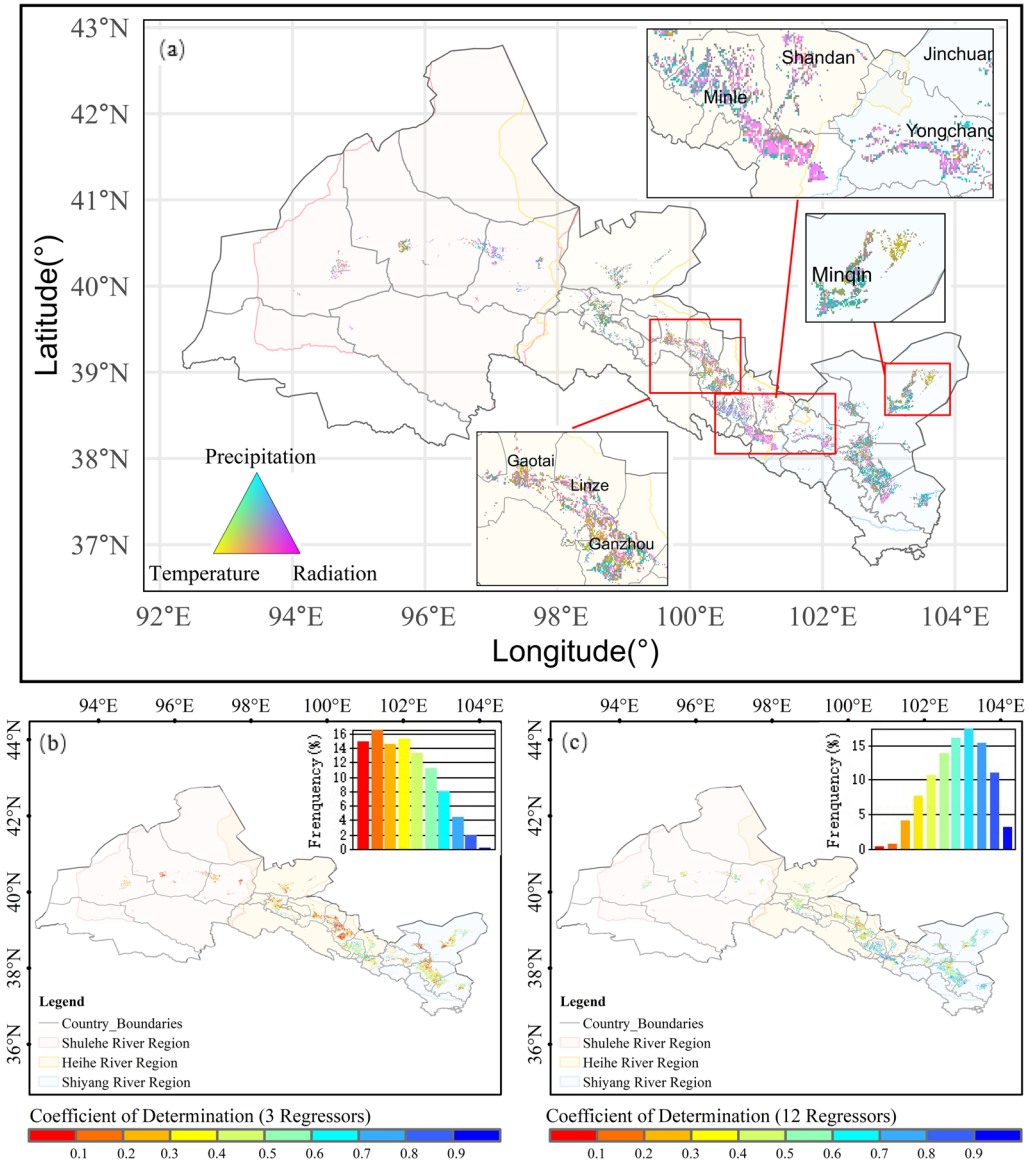

Fig. 6 **a** Cyan-magenta-yellow (CMY) triangular map of relative importance metrics. The contributions of precipitation (cyan), radiation (magenta) and temperature (yellow) to WUE IAV during 2001–2018. The coefficient of determination of multiple linear models based on **b** three regressors (precipitation, radiation and temperature) and **c** six regressors (precipitation, radiation, temperature, NDVI, soil moisture and SPEI)

of determination were improved with the addition of SPEI indices, soil moisture and NDVI data (Fig. 6c). It is indicated that these factors also played an important role on WUE IAV. The pixel-wise importance of precipitation, radiation, temperature, NDVI, SPEI and soil moisture on irrigated cropland WUE IAV shown in the Fig. 7a, the WUE IAV of 38.14% irrigated croplands was controlled by NDVI. This is because water and radiation factors can affect WUE through NDVI. SPEI and soil moisture were also the influencing factors of WUE IAV, accounting for approximately 14.2% and 7.34% of the total irrigated croplands, respectively. Meanwhile, we input all pixel values of the whole Hexi Corridor as observations in the model and the relative importance

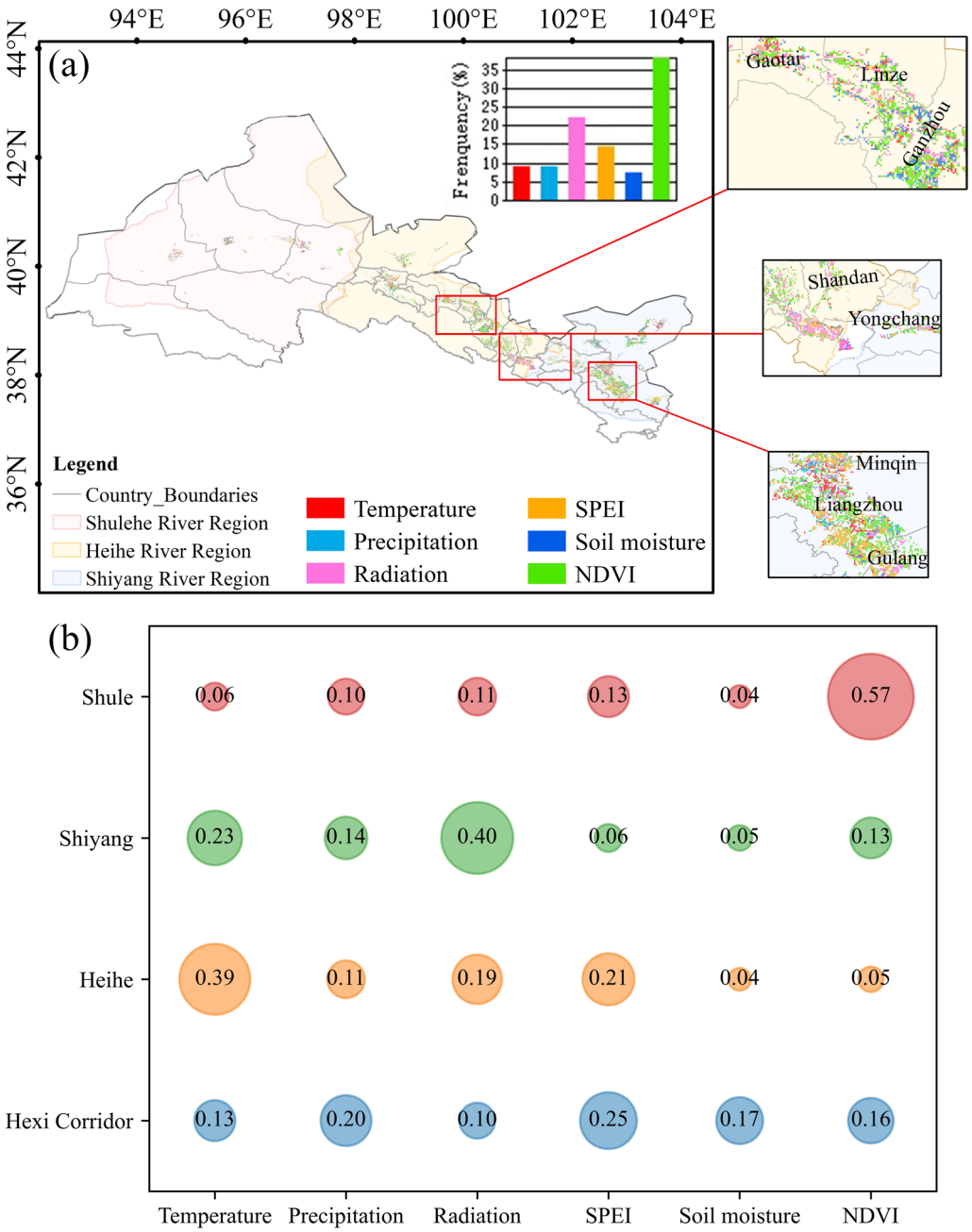

Fig. 7 The contributions of precipitation, radiation, temperature, SPEI, NDVI and soil moisture to irrigated cropland WUE IAV **a** the spatial pattern of composite map (The pixels display the climate factor with the highest relative importance metrics), and **b** the regional contribution values of among basins

metrics were normalized to sum to 1 (Fig. 7b). Overall, proportion of variance explained by model was 44.69%. SPEI demonstrated the highest relative importance (0.25) in influencing irrigated cropland WUE IAV, followed by precipitation (0.20), soil moisture (0.17), NDVI (0.16), temperature (0.13), and radiation (0.10). These findings suggest that climate-related factors accounted for less than half of the IAV changes in WUE and water-related factors were more sensitive than energy-related factors to WUE variation in the Hexi Corridor.

At the basin level, we input all pixel values of each basin area as observations in the model (Fig. 7b). The dominant factors varied among different basins. The dominant driver of WUE IAV was temperature in the Heihe River basin while radiation dominated WUE IAV in the Shiyang River basin. For the Shule River basin, the WUE IAV was mainly affected by NDVI.

Driving mechanism of WUE

We constructed an SEM model to illustrate four main categories of influencing factors (water, energy, NDVI and water-saving irrigation area) on WUE variability at the regional scale (see Sect. "Bayesian structural equation modeling" for method description). The standardized SEM explained 81% of the variation in irrigated cropland WUE (Fig. 8), thereinto, GPP had the highest direct effect (0.806) whereas NDVI exerted the highest indirect effect on WUE (0.325) (Table 2). Notably, energy and water-saving irrigation management had a positive indirect effect on WUE (0.033 and 0.189), but water had a negative indirect effect (− 0.033) on variation in WUE because of a higher direct effect on ET. Water mainly affected WUE indirectly via ET. NDVI was influenced by water and energy (0.047 and 0.255). These results indicated that biological factors (NDVI and GPP) were the primary factors influencing WUE variability. Apart from biological factors, water-saving irrigation measures also played an important role in increasing WUE, which had strong indirect effect than climate factors (water and energy) on variation in WUE.

Table 2 The indirect effects of water, energy, NDVI and water-saving irrigation to WUE variations for 2001–2018 in different basins

Subregions	Water	Energy	NDVI	Water-saving irrigation
Shule River	− 0.117	− 0.048	0.318	0.262
Heihe River	0.010	0.181	0.142	− 0.270
Shiyang River	0.051	0.021	0.295	0.242
Hexi Corridor	− 0.033	0.033	0.325	0.189

At the basin level, water had a wreaker positive effect on WUE IAV in the Heihe River (0.01) basin and the Shiyang River basin (0.051), while it had a negative effect in the Shule River basin (− 0.117) (Table 2). Energy showed relatively strong positive indirect effect on WUE variability in the Heihe River basin (0.181) than the Shiyang River basin (0.021), but negative indirect effect (− 0.048) in the Shule River basin. Besides, water-saving irrigation

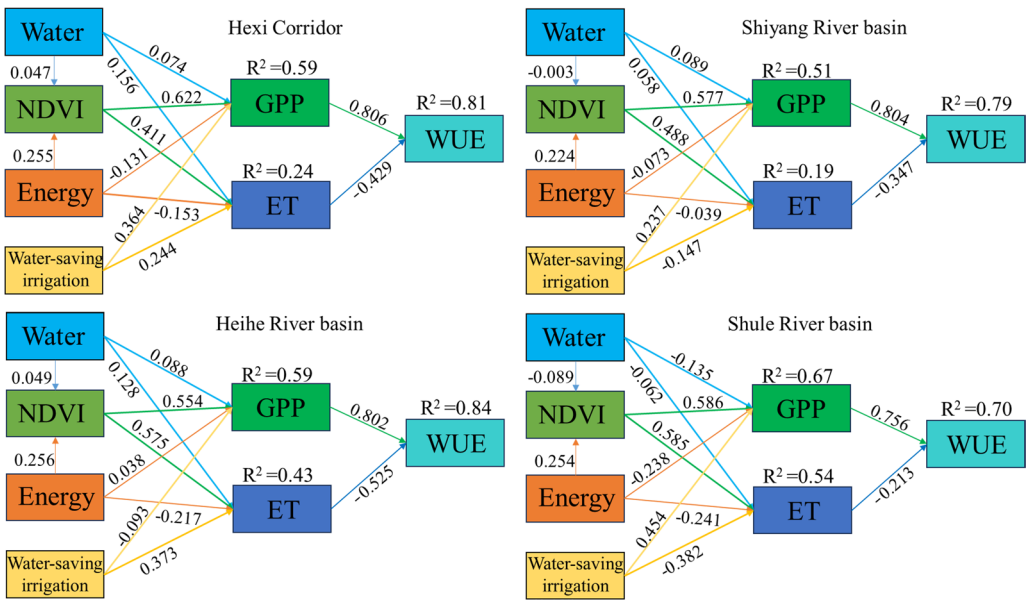

Fig. 8 Structural equation model revealing the driving mechanism of the temporal dynamics of irrigated cropland WUE based on cascade relationships in the Hexi Corridor, the Shiyang River basin, the Heihe River basin and the Shule River basin

had strong positive indirect effect on variation in WUE in the Shulehe River basin and the Shiyanghe River basin (0.262 and 0.242), which was just lower than NDVI (0.318 and 0.295). This can be attributed to positive direct effect to GPP and negative effect to ET (Fig. 8). But in the Heihe River basin, water-saving irrigation measures had negative direct effect on variation in WUE (− 0.270) because of the strong positive effect to ET.

Discussion

Comparison of WUE characteristics

In this study, the mean value of irrigated cropland WUE in the Hexi Corridor was 1.34 ± 0.38 g C kg^{-1} H_2O yr^{-1}, and WUE showed spatial heterogeneity. A study reported that global irrigated cropland WUE based on MODIS GPP and ET data was 1.62 g C kg^{-1} H_2O (Ai et al. 2020), which is higher than WUE value in this study. The study in China from Yang et al. (2022b) found the irrigated croplands in the Gansu-Xinjiang area had the lowest WUE values, but in the Huang–Huai–Hai Plain croplands with irrigation produced the highest WUE. We further compared WUE values with the regional study. Tian et al. (2020) found that the mean annual cropland WUE in the Shiyang River Basin from 2000 to 2014 was 1.575 g C kg^{-1} H_2O yr^{-1}, higher than our result in the Shiyang River Basin (1.29 ± 0.36 g C kg^{-1} H_2O yr^{-1}). A possible reason for the lower value in our study is that we extracted the WUE of the irrigated area. The rainfed croplands usually had higher WUE than irrigated croplands (Ai et al. 2020). Besides, this study found the Heihe River basin had the highest WUE, followed by the Shiyang River basin and Shule River basin. Based on the composition of major crop planting areas among the three basins (Figure S2), we found the Heihe River basin has the highest rate of corn cultivation, with maize being identified as the most water-efficient crop (Mbava et al. 2020). Our result also showed the relatively high WUE (> 1.6 g C kg^{-1} H_2O yr^{-1}) in Linze County, Gaotai County, Suzhou and Liangzhou District. This is consistent with the study by Niu et al. (2018), which found that areas of high crop WUE occurred in the Gaotai and Linze Counties based on the Soil and Water Assessment Model (SWAT).

This study demonstrated that the majority of irrigated cropland area WUE had a positive trend during 2001–2018 and larger increasing trends of WUE mainly occurred in middle reaches of the Heihe River basin (Shandan County, Minle County, Ganzhou District) and Shiyang River basin (Jinchuan County, Gulang County). A previous study detected an increasing pattern of cropland WUE in the Shiyang River basin during the period of 2000–2014, and the relative increase occurred mostly in the middle and lower oasis (Tian and Zhang 2020; Tian et al. 2020). Besides, WUE underwent a significant shift in 2011 and interannual change was larger in the second stage (2001–2011) than the first stage (2011–2018) in this study. Tian and Zhang's (2020) study also indicated that the cropland WUE time series in the Shiyang River basin increased more during 2011–2014 than during 2006–2010 as the first stage of water-saving projects (Shiyang River Basin Management Plan) including Hongyashan and 7 other irrigation districts completed by 2010. Apart of that, for the Shule River basin, Comprehensive Planning of Rational Utilization of Water Resources and Ecological Protection in Dunhuang from 2011 to 2020 gradually completed water-saving transformation in irrigation district. For the Heihe River basin, Ecological Water Transfer Project from 2000 to 2015 implemented water-efficient agricultural practices (Huang et al. 2017). It appears that the relative increase after 2011 is attributed to the implementation of water-saving projects.

Driving process of irrigated cropland WUE

In general, the contribution of GPP to WUE trends and WUE IAV was greater than that of ET. This is consistent with the findings of Wang et al. (2018b), which indicated that the IAV of WUE in cropland ecosystems was primarily attributed to GPP, based on data from several typical crop flux tower sites. Yang et al. (2022a) also found that GPP dominated the increase in WUE in Northwest China in terms of the directly influencing factors. However, Tian and Zhang (2020) found cropland WUE in the Shiyang River basin was mainly controlled by ET rather than GPP based on MODIS products. A low correlation between WUE and GPP was also observed in their study, which probably because of underestimation of MOD17 GPP in cropland (Tian and Zhang 2020). Site-level evaluation of MOD17 GPP based on eddy covariance measured GPP indicated that MODIS underestimated cropland GPP (Liu et al. 2014; Turner et al. 2005).

The dominant climatic factors of WUE IAV in irrigated croplands varied greatly across the Hexi Corridor. Apart from temperature, precipitation and radiation, SPEI and NDVI had significant effects on WUE IAV. Overall, multiple linear models based on climatic variables explained 44.69% of cropland WUE IAV, supporting the general assertion that agricultural management practices such as agricultural inputs and irrigation efficiency have a greater impact on the variations of cropland WUE than climatic factors (Sun et al. 2017). At the basin level, WUE IAV is dominated by temperature in the Heihe River basin, which is consistent with the previous study that maximum temperature dominated the crop WUE variations in the Heihe River basin, especially at the long-term scales (Niu et al. 2018).

In contrast to studies focusing solely on individual influencing factors affecting water use efficiency (WUE), the structural equation model considered a comprehensive relationship about ecosystem to introduce drivers on WUE systematically and distinguish direct and indirect effects. Apart from the climatic variables, the irrigation practice in the field, particularly water-saving irrigation measures, played important roles in improving irrigated cropland WUE (Du et al. 2010; Farooq et al. 2019; Li et al. 2016). Thus, our SEM considers the effect of irrigation management on WUE variations by integrating the water-saving irrigation area. The results found that GPP was the dominant direct factor and NDVI was the dominant indirect factor of WUE variability. This is consistent with the study conducted in China using flux site data, which found that biological factors (leaf area index (LAI), fractional vegetation coverage (FVC) and GPP) were the primary factors influencing WUE variability (Dou et al. 2024). Besides, water-saving irrigation exerted a stronger effect than water and energy in the Hexi Corridor. The significant positive effect of water-saving irrigation on cropland WUE was observed in the Shiyang River basin and the Shule River basin whereas the negative case was found in the Heihe River basin. The negative impact of water-saving irrigation on WUE in the Heihe River basin was mainly due to the strong positive effect to ET. Irrigation water losses from evaporation tend to decrease WUE. This indicated there remained water-saving irrigation potential to improve the WUE in the Heihe River basin, and less water should be supplied to maintain a relatively high WUE, without reducing crop GPP. Liu and Song (2020) found that water consumption by the crop far exceeded the actual water requirement in the Heihe River basin.

Analysis of uncertainty

In this study, WUE was derived by GPP data from EF-LUE model and ET data from ETMonitor model. Compared with WUE data calculated from the MODIS GPP and ET, ETMonitor ET demonstrates superior performance in irrigated croplands (Zheng et al. 2022, 2023), and EF-LUE GPP proves to be more effective in capturing significant negative GPP anomalies during drought or heat-wave events (Du et al. 2022). Nevertheless, there are still some uncertainties in cropland WUE estimation from GPP and ET model structure and input data. Moreover, both GPP and ET model did not integrate agronomic practices like irrigation and fertilizer application. These indices directly or indirectly affect the range of WUE. Additionally, we calculated WUE without distinguishing the types of crops and accumulated annual WUE over a full year rather than just during growing seasons. This was due to insufficient information regarding crop types, planting, and harvesting times, all of which could introduce bias in estimating WUE for irrigated croplands. Apart from that, the study tried to consider possible influencing factors like climatic factors and water-saving irrigation measures, but some limitations still exist. For example, we did not consider the effects of other environmental factors including rising CO_2, N deposition on WUE changes and changes in planting structure. Besides, water-saving measures were not considered in the pixel relative importance reanalysis because we just obtained statistic water-saving irrigation area data at the basin level rather than pixel level.

Conclusions

This study evaluated the spatial-temporal dynamics of irrigated cropland WUE and its driving factors in the Hexi Corridor during 2001–2018. The average annual WUE of irrigated cropland WUE varied from 0.07 g C kg^{-1} H_2O yr^{-1} to 2.42 g C kg^{-1} H_2O yr^{-1}, with mean value of 1.34 ± 0.38 g C kg^{-1} H_2O yr^{-1}. The temporal dynamics of WUE exhibited significantly increasing trends in most areas, with a faster growth observed during 2011–2018 compared to 2001–2010, primarily due to water-saving projects. Overall, GPP contributed more to WUE trends and IAV than ET across most of the Hexi Corridor. Climatic variables including temperature, precipitation and radiation, SPEI and NDVI explained 44.69% of cropland WUE IAV. SPEI, precipitation, and soil moisture were the three dominant factors of WUE IAV in the Hexi Corridor. Additionally, the standardized SEM based on water, energy, NDVI, water-saving irrigation area explained 81% of the variation in irrigated cropland WUE. Biological factors (NDVI and GPP) were the primary factors influencing WUE variability. Water-saving irrigation measures had strong indirect effect than climate factors (water and energy) on variation in WUE. The significant positive effect of water-saving irrigation on cropland WUE was observed in the Shiyang River basin and the Shule River basin whereas the negative case was found in the Heihe River basin. These findings offer valuable theoretical insights into the mechanisms governing the interaction between carbon and water of irrigated croplands and guide the management of water resources and land in agricultural practices within the Hexi Corridor. However, further research is needed to explore the effects of other environmental factors such as rising CO_2 levels and nitrogen deposition, as well as planting structure, on changes in WUE.

Abbreviations

WUE	Water use efficiency
GPP	Gross primary productivity
ET	Evapotranspiration
IAV	Interannual variability
SEM	Structural equation model

SPEI	Standardized precipitation evapotranspiration index
NDVI	Normalized Difference Vegetation Index
DSR	Downward Shortwave Radiation
GLASS	Global Land Surface Satellite
ESA-CCI	European Space Agency-Climate Change Initiative
CFMD	China Meteorological Forcing Dataset
GLDAS	Global Land Data Assimilation System
LMG	Lindeman–Merenda–Gold
MCMC	Markov chain Monte Carlo
SWAT	Soil and Water Assessment Model
CMY	Cyan-magenta-yellow

Supplementary Information

The online version contains supplementary material available at https://doi.org/10.1186/s13717-024-00553-1.

Supplementary Material 1.

Acknowledgements
Authors thank data providers and platforms. Acknowledgement for the data support from "National Earth System Science Data Center, National Science & Technology Infrastructure of China. (http://www.geodata.cn)".

Author contributions
Dandan Du: writing—original draft, methodology, software, visualization, conceptualization. Bo Dong: writing—review & editing, funding acquisition, project administration, supervision, conceptualization. Rui Zhang: resources, funding acquisition, methodology. Shiai Cui: writing—review & editing, software, formal analysis. Guangrong Chen: writing—review & editing, funding acquisition, formal analysis. Fengfeng Du: writing—review & editing, visualization, formal analysis.

Funding
This paper was supported by the National Key Research and Development Program of China (2021YFD190070406), the Key Research and Development Program of Gansu Province (20YF8NA107), and Agricultural Science and Technology Special Project of Gansu Province (GNKJ-2021–32).

Availability of data and materials
Data will be made available on request.

Declarations

Ethics approval and consent to participate
Not applicable.

Consent for publication
Not applicable.

Competing interests
The authors declare that they have no competing interests.

Author details
[1]Dryland Agriculture Institute, Gansu Academy of Agricultural Sciences, Lanzhou 730070, China. [2]Key Laboratory of Efficient Utilization of Water in Dry Farming of Gansu Province, Lanzhou 730070, China. [3]Key Laboratory of Low-Carbon Green Agriculture in Northwestern China, Ministry of Agriculture and Rural Affairs, Yangling 712100, China. [4]The Joint Key Laboratory of Ministry of Agriculture and Rural Affairs-Gansu Province for Crop Drought Resistance, Yield Increment and Rainwater Efficient Utilization On Rainfed Area, Lanzhou 730070, China. [5]College of Water Conservancy and Hydropower Engineering, Gansu Agricultural University, Lanzhou 730070, China. [6]Aerospace Information Research Institute, Chinese Academy of Sciences, Beijing 100101, China. [7]Institute of Botany, Jiangsu Province and Chinese Academy of Sciences, Nanjing 210014, China.

Received: 15 July 2024 Accepted: 20 September 2024
Published online: 29 September 2024

References

Ai Z, Wang Q, Yang Y, Manevski K, Yi S, Zhao X (2020) Variation of gross primary production, evapotranspiration and water use efficiency for global croplands. Agric For Meteorol 287:107935
Bai Y, Zha T, Bourque CPA, Jia X, Ma J, Liu P, Yang R, Li C, Du T, Wu Y (2020) Variation in ecosystem water use efficiency along a southwest-to-northeast aridity gradient in China. Ecol Indic 110:105932
Bao C, Fang CL (2007) Water resources constraint force on urbanization in water deficient regions: a case study of the Hexi Corridor, arid area of NW China. Ecol Econ 62:508–517
Bonan GB (2008) Forests and climate change: forcings, feedbacks, and the climate benefits of forests. Science 320:1444–1449
Didan K, Barreto Munoz A., MODIS Vegetation Index User's Guide Version 3.10. 2019. NASA LP DAAC. Available online: https://lpdaac.usgs.gov/documents/621/MOD13_User_Guide_V61.pdf. Accessed 14 Mar 2024
Dou X, Yu G, Chen Z, Yang M, Hao T, Han L, Liu Z, Ma L, Lin Y, Zhu X, Zhang W, Sun M, Luo W, Li J, Lin Q, Zhou W (2024) High spatial variability in water use efficiency of terrestrial ecosystems throughout China is predominated by biological factors. Agric For Meteorol 345:109834
Du T, Kang S, Sun J, Zhang X, Zhang J (2010) An improved water use efficiency of cereals under temporal and spatial deficit irrigation in north China. Agric Water Manag 97:66–74
Du D, Zheng C, Jia L, Chen Q, Jiang M, Hu G, Lu J (2022) Estimation of global cropland gross primary production from satellite observations by integrating water availability variable in light-use-efficiency model. Remote Sens 14:1722
Fan T, Wang S, Li Y, Yang X, Li S, Ma M (2019) Film mulched furrow-ridge water harvesting planting improves agronomic productivity and water use efficiency in rainfed areas. Agric Water Manag 217:1–10
FAO (2021) The state of the world's land and water resources for food and agriculture: systems at breaking point. FAO United Nations. Rome, Italy
Farooq M, Hussain M, Ul-Allah S, Siddique KHM (2019) Physiological and agronomic approaches for improving water-use efficiency in crop plants. Agric Water Manag 219:95–108
Feng Q, Miao Z, Li Z, Li J, Si J, Yonghong S, Chang S (2015) Public perception of an ecological rehabilitation project in inland river basins in northern China: success or failure. Environ Res 139:20–30
Feng Q, Yang L, Deo RC, AghaKouchak A, Adamowski JF, Stone R, Yin Z, Liu W, Si J, Wen X, Zhu M, Cao S (2019) Domino effect of climate change over two millennia in ancient China's Hexi Corridor. Nat Sustain 2:957–961
Fischer RA, Turner NC (1978) Plant productivity in the arid and semiarid zones. Annu Rev Plant Biol 29:277–317
GPWRB (2007) The comprehensive treatment program of Shiyang River Basin (in Chinese). Lanzhou
Grafton RQ, Pittock J, Davis R, Williams J, Fu G, Warburton M, Udall B, McKenzie R, Yu X, Che N, Connell D, Jiang Q, Kompas T, Lynch A, Norris R, Possingham H, Quiggin J (2013) Global insights into water resources, climate change and governance. Nat Clim Chang 3:315–321
Groemping U (2006) Relative importance for linear regression in R: the package relaimpo. J Stat Softw 17:1–27
HBGP (2019) Water Resources Bulletin of Gansu Province. Lanzhou
He J, Yang K, Tang W, Lu H, Qin J, Chen Y, Li X (2020) The first high-resolution meteorological forcing dataset for land process studies over China. Sci Data 7:25
Hu G, Jia L (2015) Monitoring of evapotranspiration in a semi-arid inland river basin by combining microwave and optical remote sensing observations. Remote Sens 7:3056–3087
Hu X, Lei H (2021) Fifteen-year variations of water use efficiency over a wheat-maize rotation cropland in the north China plain. Agric For Meteorol 306:108430
Huang M, Piao S, Sun Y, Ciais P, Cheng L, Mao J, Poulter B, Shi X, Zeng Z, Wang Y (2015) Change in terrestrial ecosystem water-use efficiency over the last three decades. Glob Chang Biol 21:2366–2378

Huang S, Feng Q, Lu Z, Wen X, Deo RC (2017) Trend analysis of water poverty index for assessment of water stress and water management polices: a case study in the Hexi Corridor, China. Sustainability 9:756
Ji Y, Zeng S, Tang Q, Yan L, Wu S, Fan Y, Chen J (2023) Spatiotemporal variations and driving factors of China's ecosystem water use efficiency. Ecol Indic 148:110077
Kang S, Hao X, Du T, Tong L, Su X, Lu H, Li X, Huo Z, Li S, Ding R (2017) Improving agricultural water productivity to ensure food security in China under changing environment: from research to practice. Agric Water Manag 179:5–17
Keenan TF, Hollinger DY, Bohrer G, Dragoni D, Munger JW, Schmid HP, Richardson AD (2013) Increase in forest water-use efficiency as atmospheric carbon dioxide concentrations rise. Nature 499:324–327
Lee SY, Song XY (2014) Bayesian structural equation model. Wires Comput Stat 6:276–287
Li X, Zhang X, Niu J, Tong L, Kang S, Du T, Li S, Ding R (2016) Irrigation water productivity is more influenced by agronomic practice factors than by climatic factors in Hexi Corridor, Northwest China. Sci Rep 6:37971
Lindeman RH, Merenda PF, Gold RZ (1981) Introduction to bivariate and multivariate analysis. Scott, Foresman and Company, Glenview, Illinois
Linderson ML, Mikkelsen TN, Ibrom A, Lindroth A, Ro-Poulsen H, Pilegaard K (2012) Up-scaling of water use efficiency from leaf to canopy as based on leaf gas exchange relationships and the modeled in-canopy light distribution. Agric For Meteorol 152:201–211
Liu Y, Song W (2020) Modelling crop yield, water consumption, and water use efficiency for sustainable agroecosystem management. J Clean Prod 253:119940
Liu Z, Shao Q, Liu J (2014) The performances of MODIS-GPP and -ET products in China and their sensitivity to input data (FPAR/LAI). Remote Sens 7:135–152
Liu Y, Xiao J, Ju W, Zhou Y, Wang S, Wu X (2015) Water use efficiency of China's terrestrial ecosystems and responses to drought. Sci Rep 5:13799
Mbava N, Mutema M, Zengeni R, Shimelis H, Chaplot V (2020) Factors affecting crop water use efficiency: a worldwide meta-analysis. Agric Water Manag 228:105878
Niu J, Liu Q, Kang S, Zhang X (2018) The response of crop water productivity to climatic variation in the upper-middle reaches of the Heihe river basin, northwest China. J Hydrol 563:909–926
Pan X, Zhang H, Yu S, Deng H, Chen X, Zhou C, Li F (2024) Strategies for the management of water and nitrogen interaction in seed maize production; a case study from China Hexi Corridor oasis agricultural area. Agric Water Manag 292:108685
Peng S, Ding Y, Liu W, Li Z (2019) 1 km monthly temperature and precipitation dataset for China from 1901 to 2017. Earth Syst Sci Data 11:1931–1946
Reichstein M, Ciais P, Papale D, Valentini R, Running S, Viovy N, Cramer W, Granier A, Ogée J, Allard V, Aubinet M, Bernhofer C, Buchmann N, Carrara A, Grüwald T, Heimann M, Heinesch B, Knohl A, Kutsch W, Loustau D, Manca G, Matteucci G, Miglietta F, Ourcival JM, Pilegaard K, Pumpanen J, Rambal S, Schaphoff S, Seufert G, Soussana JF, Sanz MJ, Vesala T, Zhao M (2007) Reduction of ecosystem productivity and respiration during the European summer 2003 climate anomaly: a joint flux tower, remote sensing and modelling analysis. Glob Chang Biol 13:634–651
Sen PK (1968) Estimates of the regression coefficient based on Kendall's Tau. J Am Stat Assoc 63:1379–1389
Sriwongsitanon N, Suwawong T, Thianpopirug S, Williams J, Jia L, Bastiaanssen W (2020) Validation of seven global remotely sensed ET products across Thailand using water balance measurements and land use classifications. J Hydrol Reg Stud 30:100709
Su YZ, Zhao WZ, Su PX, Zhang ZH, Wang T, Ram R (2007) Ecological effects of desertification control and desertified land reclamation in an oasis–desert ecotone in an arid region: a case study in Hexi Corridor, northwest China. Ecol Eng 29:117–124
Sun Y, Piao S, Huang M, Ciais P, Zeng Z, Cheng L, Li X, Zhang X, Mao J, Peng S, Poulter B, Shi X, Wang X, Wang YP, Zeng H (2015) Global patterns and climate drivers of water-use efficiency in terrestrial ecosystems deduced from satellite-based datasets and carbon cycle models. Glob Ecol Biogeogr 25:311–323
Sun S, Zhang C, Li X, Zhou T, Wang Y, Wu P, Cai H (2017) Sensitivity of crop water productivity to the variation of agricultural and climatic factors: a study of Hetao irrigation district, China. J Clean Prod 142:2562–2569
Sun S, Song Z, Wu X, Wang T, Wu Y, Du W, Che T, Huang C, Zhang X, Ping B, Lin X, Li P, Yang Y, Chen B (2018) Spatio-temporal variations in water use efficiency and its drivers in China over the last three decades. Ecol Indic 94:292–304
Tian F, Zhang Y (2020) Spatiotemporal patterns of evapotranspiration, gross primary productivity, and water use efficiency of cropland in agroecosystems and their relation to the water-saving project in the Shiyang river basin of northwestern China. Comput Electron Agric 172:105379
Tian F, Zhang Y, Lu S (2020) Spatial-temporal dynamics of cropland ecosystem water-use efficiency and the responses to agricultural water management in the Shiyang river basin, northwestern China. Agric Water Manag 237:106176
Turner DP, Ritts WD, Cohen WB, Maeirsperger TK, Gower ST, Kirschbaum AA, Running SW, Zhao M, Wofsy SC, Dunn AL, Law BE, Campbell JL, Oechel WC, Kwon HJ, Meyers TP, Small EE, Kurc SA, Gamon JA (2005) Site-level evaluation of satellite-based global terrestrial gross primary production and net primary production monitoring. Glob Chang Biol 11:666–684
Wang Y, Zhou B, Qin D, Wu J, Gao R, Song L (2017) Changes in mean and extreme temperature and precipitation over the arid region of northwestern China: observation and projection. Adv Atmos Sci 34:289–305
Wang T, Tang X, Zheng C, Gu Q, Wei J, Ma M (2018a) Differences in ecosystem water-use efficiency among the typical croplands. Agric Water Manag 209:142–150
Wang Y, Zhou L, Ping X, Jia Q, Li R (2018b) Ten-year variability and environmental controls of ecosystem water use efficiency in a rainfed maize cropland in northeast China. Field Crop Res 226:48–55
Wang L, Li M, Wang J, Li X, Wang L (2020) An analytical reductionist framework to separate the effects of climate change and human activities on variation in water use efficiency. Sci Total Environ 727:138306
Wang H, Li X, Xiao J, Ma M (2021) Evapotranspiration components and water use efficiency from desert to alpine ecosystems in drylands. Agric For Meteorol 298–299:108283
Weerasinghe I, Bastiaanssen W, Mul M, Jia L, van Griensven A (2020) Can we trust remote sensing evapotranspiration products over Africa? Hydrol Earth Syst Sci 24:1565–1586
Wilcox RR (2010) Fundamentals of modern statistical methods: substantially improving power and accuracy. Springer, New York
Wong DW, Yuan L, Perlin SA (2004) Comparison of spatial interpolation methods for the estimation of air quality data. J Expo Sci Environ Epidemiol 14:404–415
United Nations (2021) The United Nations world water development report 2021: valuing water. UNESCO, Paris
Xia H, Zhao X, Jiao W, Zhao W (2023) High-resolution SPEI dataset for drought monitoring and impact analysis in mainland China from 2001 to 2020. National Ecosystem Data Bank
Xu M, Kang S, Wu H, Yuan X (2018) Detection of spatio-temporal variability of air temperature and precipitation based on long-term meteorological station observations over Tianshan mountains, central Asia. Atmos Res 203:141–163
Yan P, Fernandez-Martinez M, Van Meerbeek K, Yu G, Migliavacca M, He N (2023) The essential role of biodiversity in the key axes of ecosystem function. Glob Chang Biol 29:4569–4585
Yang H, Yang D (2012) Climatic factors influencing changing pan evaporation across China from 1961 to 2001. J Hydrol 414–415:184–193
Yang L, Feng Q, Adamowski JF, Deo RC, Yin Z, Wen X, Tang X, Wu M (2020) Causality of climate, food production and conflict over the last two millennia in the Hexi Corridor, China. Sci Total Environ 713:136587
Yang L, Feng Q, Wen X, Barzegar R, Adamowski JF, Zhu M, Yin Z (2022a) Contributions of climate, elevated atmospheric CO_2 concentration and land surface changes to variation in water use efficiency in northwest China. Catena 213:106220
Yang S, Zhang J, Wang J, Zhang S, Bai Y, Shi S, Cao D (2022b) Spatiotemporal variations of water productivity for cropland and driving factors over China during 2001–2015. Agric Water Manag 262:107328
Yang L, Feng Q, Lu T, Adamowski JF, Yin Z, Hatami S, Zhu M, Wen X (2023) The response of agroecosystem water use efficiency to cropland change in northwest China's Hexi Corridor. Agric Water Manag 276:108062
Yao Y, Wang X, Li Y, Wang T, Shen M, Du M, He H, Li Y, Luo W, Ma M, Ma Y, Tang Y, Wang H, Zhang X, Zhang Y, Zhao L, Zhou G, Piao S (2017) Spatiotemporal pattern of gross primary productivity and its covariation with climate in China over the last 30 years. Glob Change Biol 24:184–196

Yu G, Song X, Wang Q, Liu Y, Guan D, Yan J, Sun X, Zhang L, Wen X (2007) Water-use efficiency of forest ecosystems in eastern China and its relations to climatic variables. New Phytol 177:927–937
Yu C, Huang X, Chen H, Huang G, Ni S, Wright JS, Hall J, Ciais P, Zhang J, Xiao Y, Sun Z, Wang X, Yu L (2018) Assessing the impacts of extreme agricultural droughts in China under climate and socioeconomic changes. Earth's Future 6:689–703
Zhang Z, Jiang H, Liu JX, Zhou GM, Liu SR, Zhang XY (2012) Assessment on water use efficiency under climate change and heterogeneous carbon dioxide in China terrestrial ecosystems. Procedia Environ Sci 13:2031–2044
Zhang X, Liang S, Zhou G, Wu H, Zhao X (2014) Generating global and surface satellite incident shortwave radiation and photosynthetically active radiation products from multiple satellite data. Remote Sens Environ 152:318–332
Zhang X, Liang S, Song Z, Niu H, Wang G, Tang W, Chen Z, Jiang B (2016) Local adaptive calibration of the satellite-derived surface incident shortwave radiation product using smoothing spline. IEEE Trans Geosci Remote Sens 54:1156–1169
Zhang X, Wang D, Liu Q, Yao Y, Jia K, He T, Jiang B, Wei Y, Ma H, Zhao X, Li W, Liang S (2019a) An operational approach for generating the global land surface downward shortwave radiation product from MODIS data. IEEE Trans Geosci Remote Sens 57:4636–4650
Zhang YJ, Gao H, Li YH, Wang L, Kong DS, Guo YY, Yan F, Wang YW, Lu K, Tian JW, Lu YL (2019b) Effect of water stress on photosynthesis, chlorophyll fluorescence parameters and water use efficiency of common reed in the Hexi Corridor. Russ J Plant Physiol 66:556–563
Zhang C, Dong J, Ge Q (2022) IrriMap_CN: Annual irrigation maps across China in 2000–2019 based on satellite observations, environmental variables, and machine learning. Remote Sens Environ 280:113184
Zhao A, Yu Q, Cheng D, Zhang A (2021) Spatial heterogeneity of changes in cropland ecosystem water use efficiency and responses to drought in China. Environ Sci Pollut Res 29:14806–14818
Zheng C, Jia L, Hu G, Lu J, Wang K, Li Z (2016) Global evapotranspiration derived by ETMonitor model based on earth observations. IEEE Int Geosci Remote Sens Symposium 2016:222–225
Zheng C, Jia L, Hu G (2022) Global land surface evapotranspiration monitoring by ETMonitor model driven by multi-source satellite earth observations. J Hydrol 613:128444
Zheng C, Jia L, Zhao T (2023) A 21 year dataset (2000–2020) of gap-free global daily surface soil moisture at 1 km grid resolution. Sci Data 10:139
Zhou Q, Zhang Y, Wu F (2021) Evaluation of the most proper management scale on water use efficiency and water productivity: a case study of the Heihe River Basin, China. Agric Water Manag 246:106671
Zhu Q, Jiang H, Peng C, Liu J, Wei X, Fang X, Liu S, Zhou G, Yu S (2011) Evaluating the effects of future climate change and elevated CO_2 on the water use efficiency in terrestrial ecosystems of China. Ecol Model 222:2414–2429

Publisher's Note